Proceedings of the 17th World Congress
The International Federation of Automatic Control
Seoul, Korea, July 6-11, 2008

Active Tape Steering Control System

Lu Xia, William Messner *

* *Data Storage Systems Center (DSSC), Carnegie Mellon University, Pittbsurgh, PA 15213, USA*

Abstract: Lateral tape motion (LTM) in tape drives hinders accurate servo head positioning and can cause damage to the tape. It is one of the major obstacles to developing high density, high performance tape drives. This paper presents the development an active tape steering system to reduce LTM. A robust controller is designed using the Robust Bode (RBode) Plot, which translates an robust performance criterion into boundary functions on the open-loop Bode plot of a compensated SISO system. With the RBode plot robust controllers can be directly synthesized with classical loop shaping.

1. INTRODUCTION

Magnetic tapes are widely used at the enterprise level and remain the first choice for long term archiving of large data sets such as financial records for U.S. Securities and Exchange Commission (SEC) regulations and health care records because of their low unit cost, high reliability and large volumeric capacity. The major challenges are to improve the performance in terms of the data rate, access time and reliability while incorporating higher linear and track densities and thinner tapes for greatly increased volumetric data storage capacity. Hughes [2004]

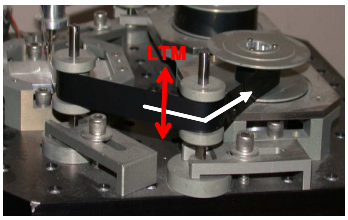

Fig. 1. Lateral Tape Motion(LTM) during tape transport.

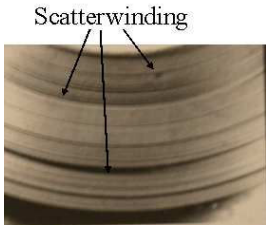

Fig. 2. Photograph of a scatter wound tape pack.

The focus of this paper is an enhancement of a conventional tape transport system to reduce lateral tape motion (LTM). LTM is the tape movement parallel to the tape plane and perpendicular to the tape transport direction (Figure 1). LTM is a major cause of the read/write head positioning error. The typical range of measured LTM in transporting one tape cartridge using a conventional tape drive is 20 microns Collins [2005]. The track density is predicted to increase from 900 tracks per inch (TPI) in 2001 to 13,000 TPI by year 2015, or less than 2 microns per track. The narrower track width substantially decreases the tolerable position error for reliable data transfer.

LTM is also a primary cause for poor tape stacking, as shown in Figure 2. The protruding tape edges are vulnerable to external damage and are the weakest parts of the tape pack. They are of great concern on maintaining the integrity and longevity of data stored on tapes Wang [2005]Collins [2004].

Conventional flanged tape guides are used to directly block excessive tape lateral motion (Figure 1). The impact between a flange and the fragile tape edge, however, could badly damage the tape edge especially during high speed tape transport. In addition to edge damage, the contact between the tape guide flange and the tape edge also excites high frequency tape lateral motion, for which the bandwidth of the head positioning system may be inadequate to keep the write-read (WR) head on the data tracks. Alternatively, rollers that have grooves between the tape guides and tape surface are used to stretch the tape surface so that the tape is kept in position by differential tension across the tape Cope et. al. [2001]. However the uneven tension itself can damage the tape, and this approach has its own limitations.

This research is motivated by the need for new technology to reduce LTM. The design concept is to detect the amount of LTM and then to actively tilt a tape guide on the tape path to shift the tape laterally. Using an active tape steering system should keep the tape within prescribed bounds, eliminating the impact with flanges during ordinary tape running.

As with most real life control systems, the active tape steering system is perturbed by modeling uncertainties, and the designed controller should maintain system performance under these uncertainties. Although automated H_∞ design tools have been widely applied in the data storage industry, they often give little insight on the relationship between the open-loop response and the closed-loop performance in the design process. Furthermore, setting

up the optimization problem may not be straightforward Green et. al. [1995]Mathwork [1995].

This paper utilizes the Robust Bode Plot (RBode Plot) developed in Lu [2005] to synthesize a robust controller. The RBode plot translates the robust performance criterion into boundary functions on the open-loop Bode plot of a SISO system to partition the plot into regions that meet the criterion and those that do not. These boundary functions incorporate both phase and magnitude information, and provide precise bounds in the entire frequency range. Subsequently, the controllers can be directly synthesized with classical loop shaping while ensuring system robust performance in presence of uncertainties and external signal perturbation.

The paper is organized as follows. Section 2 introduces the hardware design of the active tape steering system and the identified dynamics of the integrated system. Section 3 briefly introduces the RBode plot, which is then used to synthesize the robust controller by loop shaping. Experimental results on the closed loop active tape steering system appear in Section 4. Section 5 contains concluding remarks.

2. HARDWARE DESIGN AND MODELING

2.1 Hardware Design

The actuator design concept employs a tilted guide to compensate for lateral motion. To provide the tilting angle needed for lateral compensation, the guide is connected to a slanted adapter. A rotary actuator rotates the adapter as shown in Fig. 3. Rotating the integrated guide to different angular positions changes the relative tilting angle between the tape guide and the tape post causing the tape to move laterally. A rotary voice coil motor (VCM) employed

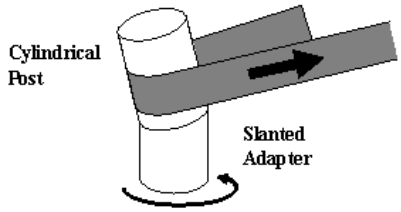

Fig. 3. The concept of the actuator design.

in disk drives serves as the rotational actuator. Figure 4 shows the tilting guide assembly. The integration of the active steering tape drive test stand is shown in Figure 5.

2.2 System Identification

A SigLab VNA dynamic signal analyzer was used to extract the characteristics of the integrated active steering tape transport system under the operating condition velocity = 4 m/s and tension = 1 N. Eight groups of system identification experiments were conducted. Figure 6 shows

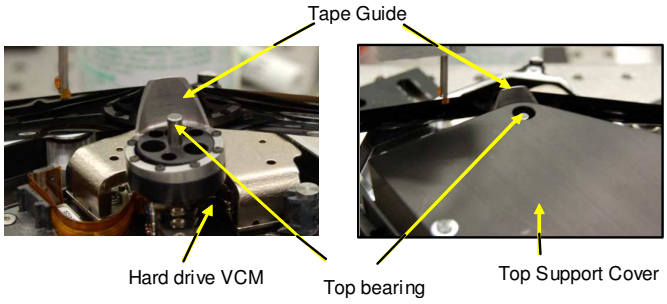

Fig. 4. Picture of the active steering actuator.

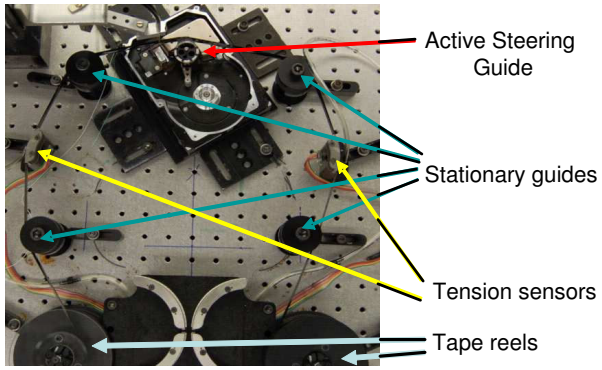

Fig. 5. The integrated hardware with second generation actuator and modified tape path.

the eight frequency response data models. The second order model

$$P_m = \frac{7.0e4}{s^2 + 593s + 4.4e4} \tag{1}$$

captures the most dominant system dynamics as indicated by the black solid cruve in Figure 6. The transfer function P_m is used as the nominal system model.

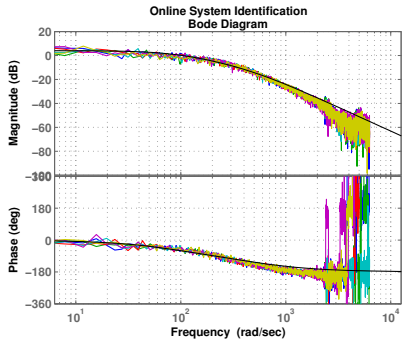

Fig. 6. Bode Diagram of the System Characteristics from online System Identification.

3. CONTROLLER DESIGN WITH THE RBODE PLOT

3.1 RBode Plot Introduction

Robust Bode plot (RBode plot) is an enhancement to the conventional Bode plot to make it a more effective tool for loop shaping. In RBode plots, boundary functions which represent performance bounds are added to the

open loop magnitude and phase plots to partition the conventional Bode plots into regions that do and do not meet specific robust performance criteria. Details of the RBode derivation can be found in Lu [2005], but a brief explanation is below.

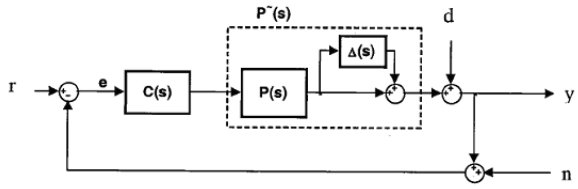

Fig. 7. Block diagram with multiplicative model uncertainty.

.

Consider the uncertain plant described by the multiplicative uncertainty model shown in Figure 7, where $\tilde{P}(s)$ is the uncertain plant, and $P(s)$ is a known transfer function representing the nominal plant. The uncertainty model, $\Delta(s)$, is an unknown but stable transfer function with $|\Delta(\jmath\omega)| < |W_u(\omega)|$, for all ω. The weighting function, $W_u(\omega)$ satisfies

$$\left|\frac{\tilde{P}(\jmath\omega)}{P(\jmath\omega)} - 1\right| \leq |W_u(\omega)|, \text{ for all } \omega,$$

where the magnitude response of $W_u(\omega)$ is an upper bound of the magnitude of the model uncertainty, $|\Delta(\jmath\omega)|$.

The desired performance of the system is specified by a weighting function $W_s(\omega)$ such that

$$|\tilde{S}(\jmath\omega)| < |W_s(\omega)|^{-1}, \text{ for all } \omega, \text{ where } \tilde{S}(s) \equiv \frac{1}{1+\tilde{P}(s)C(s)} \quad (2)$$

If the nominal loop transfer function $L(s) \equiv P(s)C(s)$ is stable, a necessary and sufficient condition for a SISO controller to achieve robust performance is Doyle [1992]

$$|W_u(\omega)T(\jmath\omega)| + |W_s(\omega)S(\jmath\omega)| = \frac{|W_u(\omega)L(\jmath\omega)| + |W_s(\omega)|}{|1+L(\jmath\omega)|} < 1 \quad (3)$$

for all frequencies ω, where $\tilde{T}(s) \equiv \frac{\tilde{P}(s)C(s)}{1+\tilde{P}(s)C(s)}$

For SISO systems, using the fact that $L = |L|cos\,(arg(L)) + j|L|sin\,(arg(L))$, inequality (3) (after suppressing ω for notational convenience) is equivalent to

$$(1-|W_u|^2)|L|^2 + 2(\cos(\arg(L)) - |W_u||W_s|)|L| + 1 - |W_s|^2 > 0. \quad (4)$$

Solving (4) for the magnitude $|L|$ defines magnitude boundary functions which are dependent on the two weighting functions and the open-loop phase response $\arg(L)$. Plotting the magnitude boundary functions and the open-loop Bode magnitude chart on the same axes generates the magnitude chart of the RBode plot.

The upper subplot of Figure 11 shows an example of an RBode magnitude plot where the system does not satisfy the robust performance criterion, because there are intersections between the open-loop magnitude response and the forbidden regions indicated by gray cross hatching. Figure 16 shows an example of an RBode magnitude plot where the system does satisfy the robust performance criterion, because there are no such intersections.

Similar boundary functions can be defined for the phase plot by rewriting (3) as

$$\cos(\arg(L)) > \frac{|W_s|^2 - 1 + 2|W_sW_u||L| + (|W_u|^2 - 1)|L|^2}{2|L|}. \quad (5)$$

Solving (5) for the phase $\arg(L)$ defines phase boundary functions which are dependent on the weighting functions and the loop magnitude response $|L|$. Plotting the phase boundary functions and the open-loop Bode phase chart on the same axes generates the phase chart of the RBode plot.

The lower subplot of Figure 11 shows an example of an RBode phase plot where the system does not satisfy the robust performance criterion, because there are intersections between the open-loop phase response and the cross hatched forbidden regions. Figure 16 shows an example of an RBode phase plot where the system does satisfy the robust performance criterion, because there are no such intersections.

The strategy for compensator design with loop shaping with the RBode plot is to shape the open-loop response to assure that the nominal loop response does not enter the forbidden region defined by boundary functions at any frequency.

3.2 Robust controller design for active tape steering system

Performance Specification Significant disturbances in various frequency ranges are observed in open-loop LTM data collected during operation of the MTS (Multi-terabyte Tape System) tape transport. Dominant disturbances originate from either tape edge imperfections or tape drive reel imperfections. Disturbances below 25 Hz are of major concern and the specifications for the closed-loop system are

(1) Zero steady state error for a constant disturbance;
(2) Disturbance attenuation below 60 Hz (382 rad/sec);
(3) At least 6 dB of attenuation for disturbances at frequencies below 24 Hz (151 rad/sec);
(4) No more than 4 dB of disturbance amplification at any frequency;

The performance weighting function for the controller synthesis is

$$W_s(\omega) = \left|\frac{0.63s + 297}{s + 40}\right|_{s=j\omega}. \quad (6)$$

Figure 8 shows the magnitude response of W_s and its reciprocal, which is the desired upper bound for the sensitivity function.

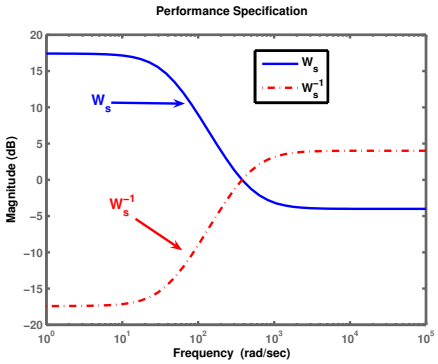

Fig. 8. Weighting function for robust performance.

Extraction of Plant Uncertainties The mismatch between the nominal model and the actual frequency response data in Figure 6 is treated as system uncertainties. The multiplicative mismatch between each frequency response data model and the nominal model is

$$P_{mismatch\_i} = \frac{P_{collected\_i}}{P_m} - 1 \tag{7}$$

Figure 9 shows the magnitude of $P_{mismatch\_1}$, $\cdots$, $P_{mismatch\_8}$.

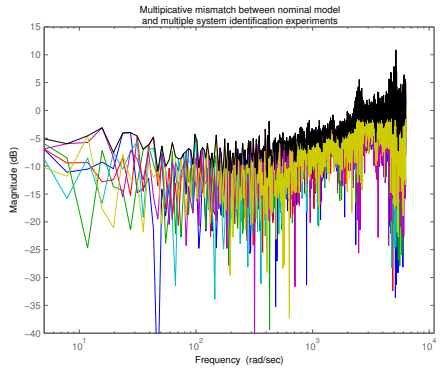

Fig. 9. Bode Diagram of the Multiplicative differences.

In traditional robust controller design such as H_∞-synthesis, the system uncertainty weighting function must be represented as a stable transfer function. There is no such requirement for generating of the RBode plot. Instead of trying to fit a transfer function to the mismatches in Figure 9 to a transfer function, we simply constructed a tentative uncertainty weighting function as another frequency response data model which represents the worst-case model mismatch observed during system identification process. That is,

$$|W_{max\_mismatch}(j\omega)| = Max_{i=1,\cdots 8}|P_{mismatch\_i}(j\omega)|, \forall\ \omega \tag{8}$$

The magnitude of $W_{max\_mismatch}(\omega)$ is shown in Figure 10 as dotted line. The maximal mismatch model, however, includes not only the real plant model variations but also perturbations on plant input and output collected during the online system identification process. As observed from Figure 10, there are a few magnitude spikes at random frequency points. Such spikes are inconsistent with known characteristics of system uncertainties and can be considered as modeling outliers. The solid line in Figure 10 shows the frequency response data model after outlier removal and is the multiplicative uncertainty weighting function $W_u(\omega)$ used for the design.

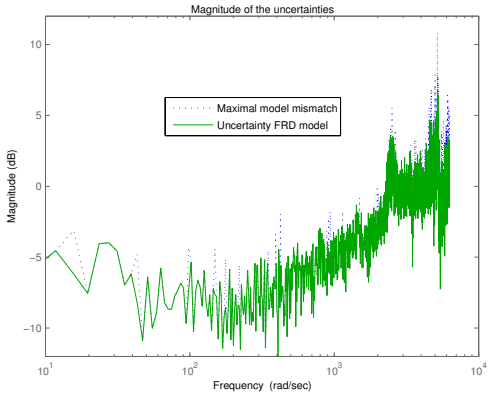

Fig. 10. The uncertainty weighting frequency response data model.

Loop shaping design using RBode plots Figure 11 shows the initial Rbode plot of the plant with no compensation. The open-loop magnitude response is inside the forbidden region of the RBode plot below 400 rads/s, indicating that simply closing the loop without compensation will achieve neither robust performance nor robust stability. Below 100 rad/sec, the yellow shaded region in the RBode phase plot shows that the current phase response could never meet the robust performance criterion and implies that the compensation must increase the low frequency gain to lie above the shaded region in the magnitude response.

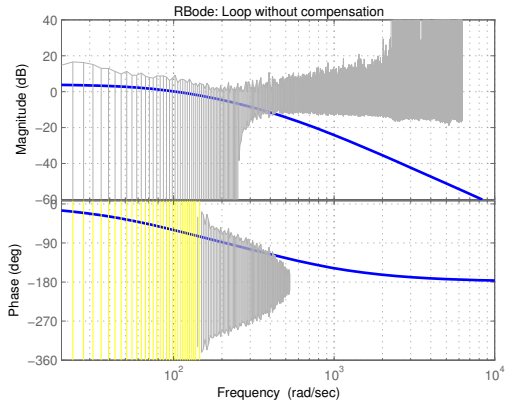

Fig. 11. The RBode plot for the open-loop with C(s)=1.

Employing the PI compensator $C_{PI}(s) = 3.16\frac{s+100}{s}$ leads to Figure 12. The compensated system still violates the robust performance criterion between 200 rad/sec and 900 rad/sec approximately. The violations of the forbidden regions shown on the phase contours suggest using a lead compensator to shift the loop phase out of the forbidden region. Applying an 80 degree complex lead compensator at 1000 rads/s with 5 dB gain and damping ratio 0.96 $C_{clead}(s) = 7.67\frac{s^2+916s+2.3e5}{s^2+4e3s+4.3e6}$ results in Figure 13.

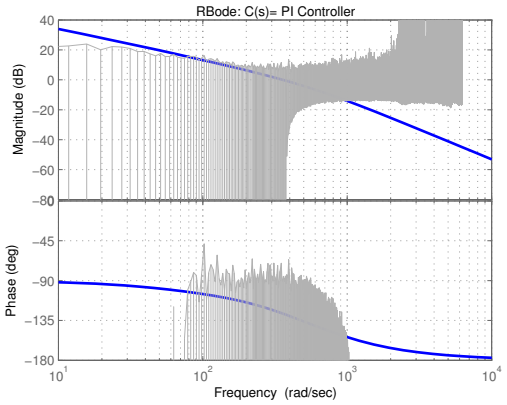

Fig. 12. RBode plot of the loop with a PI controller.

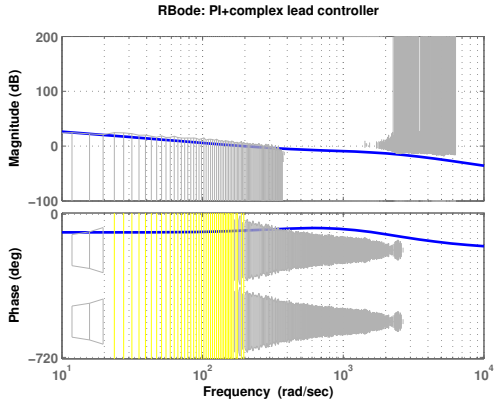

Fig. 13. RBode plot of the loop with PI and adjusted complex lead compensator.

Now the RBode plot indicates a robustness violation between 20 rad/sec and 240 rad/sec. A lag compensator can increase the gain in this frequency range. Applying $C_{clag} = 2.1\frac{s^2+45.1s+1469}{s^2+29.5s+628.5}$, which is a 40 degree complex lag compensator at 31 rad/sec with damping ratio 0.59, results in Figure 14.

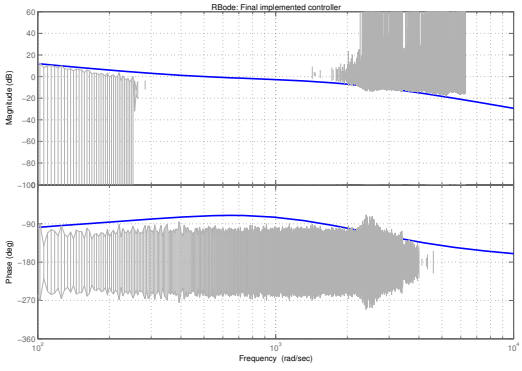

Fig. 14. RBode plot of the loop with PI+Complex Lead+Complex Lag controller.

The RBode plot of the loop compensated by the 5th order controller still shows a violation in the range 2000-3000 rad/sec. One can continue the process to design higher-order controller to achieve robust performance on the entire frequency range. Alternatively we can also reexamine the robust performance requirements based on the analysis of the disturbance spectrum. Disturbances between 2000 to 3400 rad/sec are not considered to be of concern. Therefore it is also reasonable to relax the performance specification, by changing the weighting function instead of increasing the complexity of the controller. Adding a 4 dB notch filter at 2600 rad/sec to W_s gives a relaxed performance weighting function $\bar{W}_s$ as shown in Figure 15.

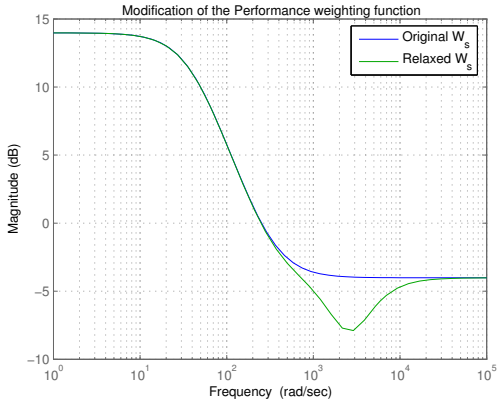

Fig. 15. Relaxed performance weighting function W_s.

Figure 16 graphs the RBode plot of the 5-th order controller with the revised performance weighting function. Based on knowledge gathered on disturbances on the tape drive, this compromise is acceptable, and the existing controller is used as the final design. The final controller used in the implementation is

$$C(s) = 50.2\frac{(s+100)(s^2+45.1s+1.5e3)(s^2+916s+2.3e5)}{s(s^2+29.5s+628.5)(s^2+4.0e3s+4.3e6)} \quad (9)$$

Note that although the order of the weighting function has increased, the order of the robust controller has not. This is in contrast to automated methods, for which the order of the synthesized controller is dependent on the order of the augmented plants.

Figure 17 shows the magnitude of $\left|\bar{W}_s S + W_u T\right|$ with respect to frequency on a log-log plot. The magnitude is below unity for all frequencies, verifying that the design satisfies the robust performance criterion. As another check, Figure 18 shows the sensitivity functions of the controlled loop are below the desired upper bound $\bar{W}_s{}^{-1}$. The sensitivity functions are frequency response data models calculated directly from the eight collected frequency response data models and the frequency response of the 5-th order controller converted from the transfer function.

4. IMPLEMENTATION

Figure 19 shows the experimental results observed under the operating condition velocity = 4 m/s and tension = 1 N. The system was sampled at 2 KHz with a zero order hold. Both open-loop and closed-loop tests collected 60

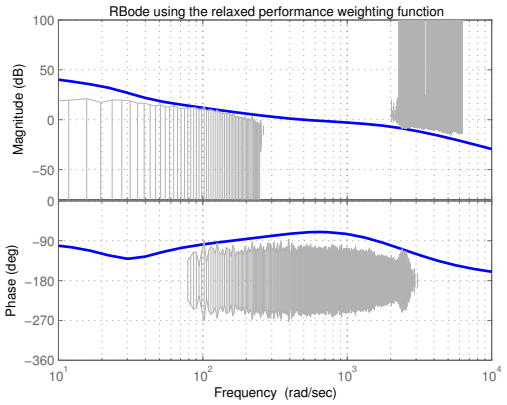

Fig. 16. RBode plot of the implemented loop, with the uncertainty weighting function and the new performance weighting function.

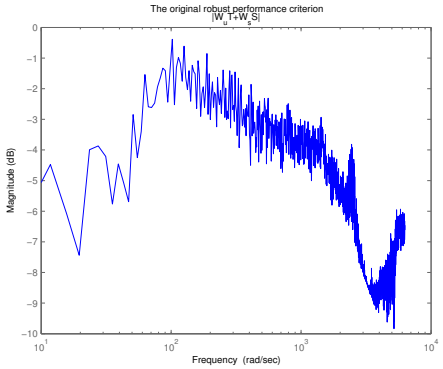

Fig. 17. Magnitude of the original robust performance criterion.

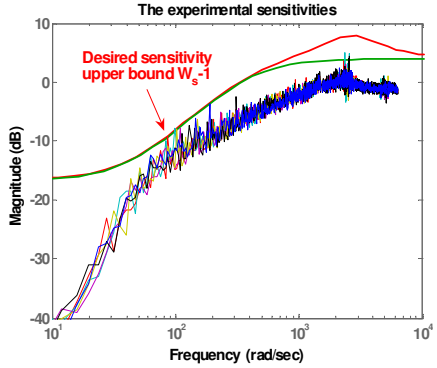

Fig. 18. Sensitivity functions corresponding to the eight FRD models compensated by the controller of (9).

seconds of data, which show the behavior of the beginning of the same tape pack. In the closed-loop test, controller function was turned on after about 12 seconds. The system exhibits a fast rise time of less than 10 ms. Figure 19 also shows the histograms for both open-loop and closed-loop LTM data, and indicating over 60% reduction in LTM.

5. CONCLUSION

This paper presented the development of an active tape steering control system to compensate for lateral tape

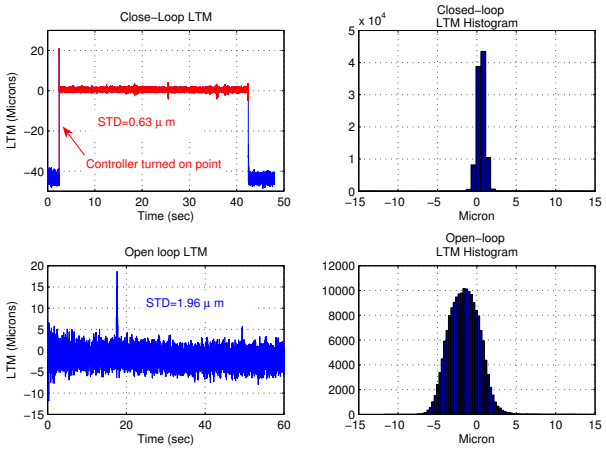

Fig. 19. LTM control system performance for tracking constant reference signal.

motion. Robust Bode plots were used to design a robust controller without a transfer function model for the uncertainty bound the dynamics. Experiments on the tape transport showed the effectiveness of the hardware design and controller design method.

ACKNOWLEDGEMENTS

This research is supported by Imation Corporation and NIST MTS funding.

REFERENCES

Hughes, G. Reliability and Security of D2D Backup Storage Systems Using SATA Drives, Technical Report. *The Information Storage Industry Center*, University of California, San Diego,March 2004

Collins,G. Measuring Small: The Technique of Measuring Very Small Lateral Tape Motion (LTM). *THIC meeting at the National Center for Atmospheric Research*, Boulder CO, June, 2005

Wang, J., et. al. Tape Edge Wear and Its Relationship to Lateral Tape Motion. *Microsystem Technologies*, vol 11, issue 8, August 2005, page 1158-1165.

Collins, G. How far can tape guide rollers go? Is a 3-piece design the future? *Computer Technology Review* March 2004.

Cope, J. R.; Zweighaft, J. Roller guiding system for delivery of tape media along a tape path United States Patent 6320727, 2001.

M. Green and D. Limebeer. *Linear Robust Control.* Prentice Hall (1995)

G.J. Balas, J. Doyle, K. Glover, A. packard, and R.Smith. *μ-Analysis and synthesis Toolbox User's guide.* The Mathworks Inc., second edition, 1995.

J. Doyle, B. Francis and A. Tannenbaum. *Feedback Control Theory.* Macmillan Publishing Company, 1992.

L. Xia. and W. Messner. Loop shaping for Robust Performance Using RBode Plot *American Control Conference* Portland, OR, 2005.